NASA TECHNICAL NOTE

NASA TN D-5090

NASA TN D-5090

COLD PERFORMANCE EVALUATION OF 4.97-INCH RADIAL-INFLOW TURBINE DESIGNED FOR SINGLE-SHAFT BRAYTON CYCLE SPACE-POWER SYSTEM

by William J. Nusbaum and Milton G. Kofskey

Lewis Research Center
Cleveland, Ohio

NATIONAL AERONAUTICS AND SPACE ADMINISTRATION • WASHINGTON, D. C. • MARCH 1969

NASA TN D-5090

COLD PERFORMANCE EVALUATION OF 4.97-INCH RADIAL-INFLOW TURBINE DESIGNED FOR SINGLE-SHAFT BRAYTON CYCLE SPACE-POWER SYSTEM

By William J. Nusbaum and Milton G. Kofskey

Lewis Research Center
Cleveland, Ohio

NATIONAL AERONAUTICS AND SPACE ADMINISTRATION

For sale by the Clearinghouse for Federal Scientific and Technical Information
Springfield, Virginia 22151 – CFSTI price $3.00

ABSTRACT

Tests were conducted in argon over a range of turbine inlet pressures from 2.95 to 16.40 psia (2.03 to 11.31 N/cm^2 abs) corresponding to a Reynolds number range from 34 950 to 175 800 at equivalent design speed and pressure ratio. Results are presented to show the effect of this change in Reynolds number on turbine performance. Results are also presented in terms of equivalent specific work, mass flow, torque, and efficiency for operation at the design Reynolds number of 76 200 and at speeds ranging from 0 to 110 percent of equivalent design speed with inlet-total- to exit-static-pressure ratios of 1.33 to 2.01.

INTRODUCTION

The Brayton space-power technology program being conducted at the NASA Lewis Research Center has included the aerodynamic study of the associated turbine components. Initial studies involved both radial and axial flow units that were sized to match the requirements of an exploratory two-shaft 10-kilowatt (electrical) nominal power system. The results of the studies (refs. 1 to 4) indicated that satisfactory efficiencies can be obtained from the small units involved, particularly in the case of the radial inflow turbine.

More recently, attention has been focused on a single-shaft Brayton power system designed for a power range from 2 to 10 kilowatts (electrical). The selected combination of rotative speed (36 000 rpm), working fluid (krypton molecular weight), pressure level, etc., were such that the resultant turbine specific speed of 76 (0.59) was in the range considered favorable for high efficiency. However the unit was somewhat smaller than that utilized in the previous program, the rotor diameter being 4.97 inches (12.62 cm). The turbine uses a helium-xenon gas mixture as the working fluid. This mixture, which has the same molecular weight as krypton, was used instead of krypton because the helium in the mixture provides better heat-transfer characteristics (ref. 5).

Because of the significance of turbine efficiency as affecting the performance of the complete Brayton Power system, it was considered important to experimentally determine the aerodynamic performance of this small radial inflow turbine. Therefore, a research model of the turbine was constructed as part of a complete package procurement and delivered to the Laboratory for evaluation.

A description of mechanical and aerodynamic design of the turbine is made in reference 6. The turbine package used air-oil-mist lubricated ball bearings to simplify the aerodynamic study, instead of gas bearings, which would be used in the actual space-power system. The investigation of the turbine was made both with and without an exit diffuser. All tests were made with argon as the working fluid at an inlet temperature of 610° R (339 K). Performance was first determined at an inlet pressure of 7.0 psia (4.8 N/cm^2) which corresponds to design Reynolds number at equivalent design speed and pressure ratio. The effect of Reynolds number on performance was then determined by operating the turbine over a range of inlet pressures from about 2.95 to 16.40 psia (2.03 to 11.31 N/cm^2 abs) with corresponding Reynolds number from 34 950 to 175 800. At each inlet pressure, data were obtained over a range of blade-jet speed ratios by varying speed and/or pressure ratio.

This report presents turbine design information and performance of the turbine with and without the exit diffuser. Test results are presented in terms of equivalent specific work, torque, mass flow, and efficiency. Included are the results of a radial survey of rotor-exit flow angle, total temperature, and total pressure at design-point of operation.

COLD PERFORMANCE EVALUATION OF 4.97-INCH RADIAL-INFLOW TURBINE DESIGNED FOR SINGLE-SHAFT BRAYTON CYCLE SPACE-POWER SYSTEM

by William J. Nusbaum and Milton G. Kofskey

Lewis Research Center

SUMMARY

A 4.97-inch (12.62-cm) radial-inflow turbine designed for a 6-kilowatt single-shaft Brayton cycle space-power system was investigated experimentally. Performance results are described for operation over a range of turbine-inlet pressures from 2.95 to 16.40 psia (2.03 to 11.31 N/cm^2 abs) corresponding to a Reynolds number range from 34 950 to 175 800 at equivalent design speed and pressure ratio and with argon as the working fluid. Tests at design Reynolds number (76 200) were made at speeds ranging from 0 to 110 percent of equivalent design speed and pressure ratios from 1.33 to 2.01.

Equivalent specific work of 15.22 Btu per pound (35.43 J/g) was obtained at approximately design Reynolds number (76 200) and at equivalent design speed and inlet-total-to rotor-exit-static-pressure ratio. The work output of the turbine was 2.7 percent greater than the design value of 14.82 Btu per pound (34.50 J/g). Equivalent design mass flow of 0.486 pound per second (0.220 kg/sec) was obtained at equivalent design point of operation.

The static and total efficiencies at design-point operation (based on turbine-inlet and rotor-exit conditions) were 0.872 and 0.913, respectively. These values are both about 0.02 greater than the respective design values. Static and total efficiencies based on diffuser exit conditions were 0.888 and 0.894. Use of a diffuser resulted in a 0.015 increase in static efficiency and a 0.02 decrease in total efficiency from those based on rotor-exit conditions. Comparison of these results with the design values indicates a poor performance of the diffuser. However, the overall performance level of the turbine was still better than design.

Both static and total efficiencies (with and without diffuser) increased by about 0.035 (at equivalent design speed and pressure ratio) as the Reynolds number increased from 34 950 to 175 800.

SYMBOLS

A	flow area, $in.^2$; cm^2
g	dimensional constant, 32.174 ft/sec^2; 9.807 m/sec^2
H	isentropic specific work (based on total pressure ratio), ft-lb/lb; J/g
Δh	specific work, Btu/lb; J/g
N	turbine speed, rpm
N_s	specific speed, $NQ^{1/2}/H^{3/4}$, $rpm(ft)^{3/4}/sec^{1/2}$; $(rad)(m)^{3/2}(kg)^{3/4}/(sec)^{3/2}(J)^{3/4}$
p	pressure, psia; N/cm^2 abs
Q	volume flow (based on exit conditions), ft^3/sec; m^3/sec
R	gas constant, $(ft\text{-}lb)/(lb)(^oR)$; $(N\text{-}m)/(kg)(K)$
Re	Reynolds number, $w/\mu r_t$
r	radius, ft; m
T	absolute temperature, ^oR; K
U	blade velocity, ft/sec; m/sec
V	absolute gas velocity, ft/sec; m/sec
V_j	ideal jet speed corresponding to total- to static-pressure ratio across turbine, ft/sec; m/sec
W	relative gas velocity, ft/sec; m/sec
w	weight flow, lb/sec; kg/sec
α	absolute gas flow angle measured from axial direction, deg
γ	ratio of specific heats
δ	ratio of inlet total pressure to U.S. standard sea-level pressure, p'/p*
ϵ	function of γ used in relating parameters to those using air inlet conditions at U.S. standard sea-level conditions, $\frac{0.740}{\gamma}\left(\frac{\gamma+1}{2}\right)^{\gamma/(\gamma-1)}$
η	turbine efficiency
η_s	static efficiency (based on inlet-total- to exit-static-pressure ratio)
η_t	total efficiency (based on inlet-total- to exit-total-pressure ratio)

θ_{cr} squared ratio of critical velocity at turbine inlet to critical velocity at U. S. standard sea-level temperature, $(V_{cr}/V^*_{cr})^2$

μ gas viscosity, lb/(ft)(sec); kg/(m)(sec)

ν blade-jet speed ratio (based on rotor-inlet tip speed), U_t/V_j

τ torque, in.-lb; N-m

Subscripts:

cr condition corresponding to Mach number of unity

eq equivalent

id ideal

u tangential component

t tip

1 station at turbine inlet (fig. 3)

2 station at stator exit

3 station at rotor exit

4 station at diffuser exit

Superscripts:

' absolute total state

* U. S. standard sea-level conditions (temperature equal to 518.67° R (288.15 K), pressure equal to 14.70 psia (10.13 N/cm^2))

TURBINE DESIGN REQUIREMENTS

As mentioned in the INTRODUCTION, the 4.97-inch (12.62-cm) tip diameter radial-inflow turbine was designed for 6.0 kilowatt net electrical output with xenon-helium mixture as the working fluid. The design-point values for the turbine are as follows:

Inlet total temperature, T_1', ^{o}R; K	2060; 1144
Inlet total pressure, p_1', psia; N/cm^2 abs	25; 17.24
Mass flow, w, lb/sec; kg/sec	0.7484; 0.3395
Turbine rotative speed, N, rpm	36 000
Total- to total-pressure ratio	
Overall, p_1'/p_4'	1.749
Rotor exit, p_1'/p_3'	1.740
Total- to static-pressure ratio	
Overall, p_1'/p_4	1.763
Rotor exit, p_1'/p_3	1.800
Blade-jet speed ratio, ν	0.690
Total to total efficiency	
Overall, $\eta_{t,1 \text{ to } 4}$	0.884
Rotor exit, $\eta_{t,1 \text{ to } 3}$	0.897
Total to static efficiency	
Overall, $\eta_{s,1 \text{ to } 4}$	0.875
Rotor exit, $\eta_{s,1 \text{ to } 3}$	0.850
Specific work, Δh, Btu/lb; J/g	21.80; 50.75
Reynolds number, $Re = w/\mu r$	76 200
Specific speed, $N_3 = NQ^{1/2}/(H)^{3/4}$ rpm$(ft^{3/4})/sec^{1/2}$; $(rad)(m^{3/2})(kg^{3/4})/(sec)^{3/2}(J)^{3/4}$	76; 0.59

The following air equivalent (U.S. standard sea level) design values were computed:

Mass flow, $\epsilon w\sqrt{\theta_{cr}}/\delta$, lb/sec; kg/sec	0.4860; 0.2204
Specific work, $\Delta h/\theta_{cr}$. Btu/lb; J/g	14.82; 34.50
Torque, $\tau\epsilon/\delta$, in.-lb; N-m	21.64; 2.44
Rotative speed, $N/\sqrt{\theta_{cr}}$, rpm	29 687
Total- to total-pressure ratio	
Overall, $(p_1'/p_4')_{eq}$	1.658
Rotor exit, $(p_1'/p_3')_{eq}$	1.645
Total- to static-pressure ratio	
Overall, $(p_1'/p_4')_{eq}$	1.669
Rotor exit, $(p_1'/p_3')_{eq}$	1.695
Blade-jet speed ratio, ν	0.690

The equivalent pressure ratios were calculated from equivalent specific work in air with the assumption of no change in efficiency when xenon-helium mixture of air is used as the working fluid. Rotor-inlet tip blade speed was used for the calculation of blade-jet speed ratio.

TURBINE DESIGN AND DESCRIPTION

Velocity Diagrams

The design turbine rotor dimensions, namely, tip diameter, tip width, exducer hub- to tip-diameter ratio, and exducer tip diameter, were obtained from calculations involving turbine efficiency and correlations based on the contractor's and other radial turbine data. With these major rotor dimensions and design conditions of pressure, temperature, mass flow, and speed, velocity diagrams were calculated to meet the design work requirement. Figure 1 shows the design velocity diagrams for conditions just inside the blade row. The figure shows the rotor relative inlet angles that result in minimum rotor incidence losses. The diagrams show subsonic flow throughout the turbine. The figure also shows that the turbine was designed with approximately zero exit whirl. Further description of the velocity diagrams and turbine design can be found in reference 6.

Stator Blades

In the design of the stator, the blade shape and the number of blades were optimized for minimum friction and mixing losses by use of boundary-layer techniques.

The design resulted in 13 stator blades equally spaced. The chord length of the stator blades was 1.800 inches (4.572 cm).

Rotor Blades

In the design of the rotor, the blade shape and the number of blades were optimized for low losses. Splitter vanes are used over the initial two-thirds of the rotor. The resultant decrease in loading is required at the hub to prevent low-blade-surface velocities. The final design resulted in the rotor having 11 blades and 11 splitter vanes.

The blade surface velocity distributions at design operation are shown in figure 2. These were calculated at Lewis with the method described in reference 7. These veloc-

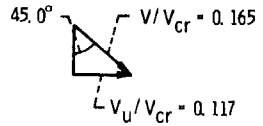

Stator inlet

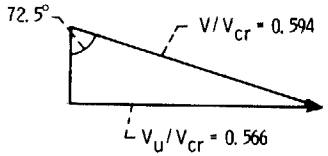

Stator exit

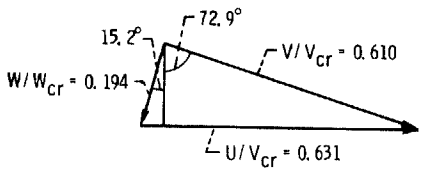

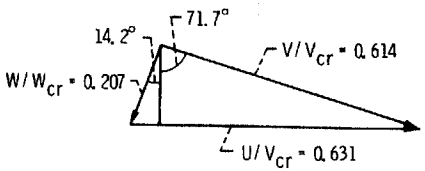

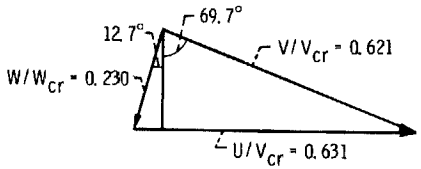

Rotor inlet

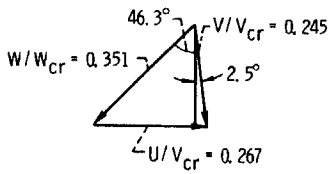

(a) Hub.

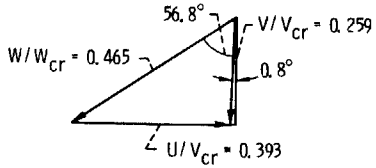

(b) 50-Percent streamline.

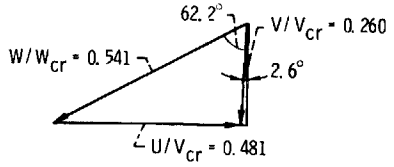

(c) Shroud.

Rotor exit

Figure 1. - Design velocity diagrams (inside blade row).

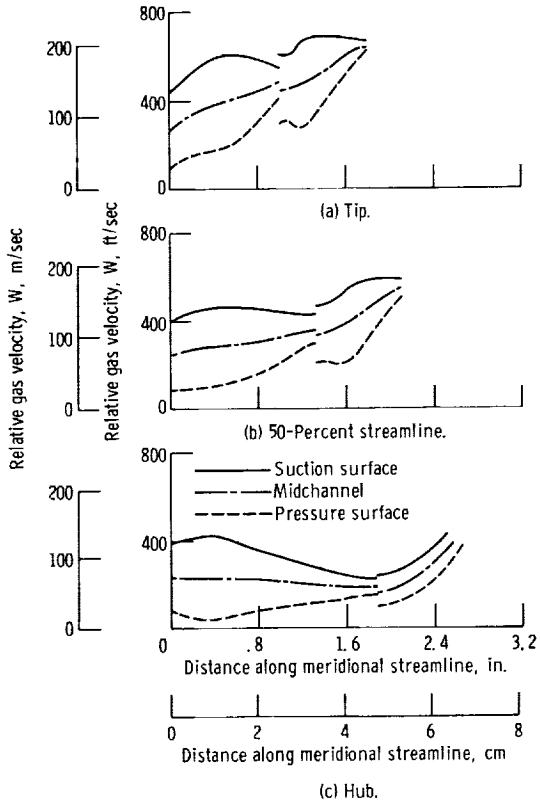

Figure 2. - Calculated rotor-blade midchannel and blade surface velocity distributions for design-point operation.

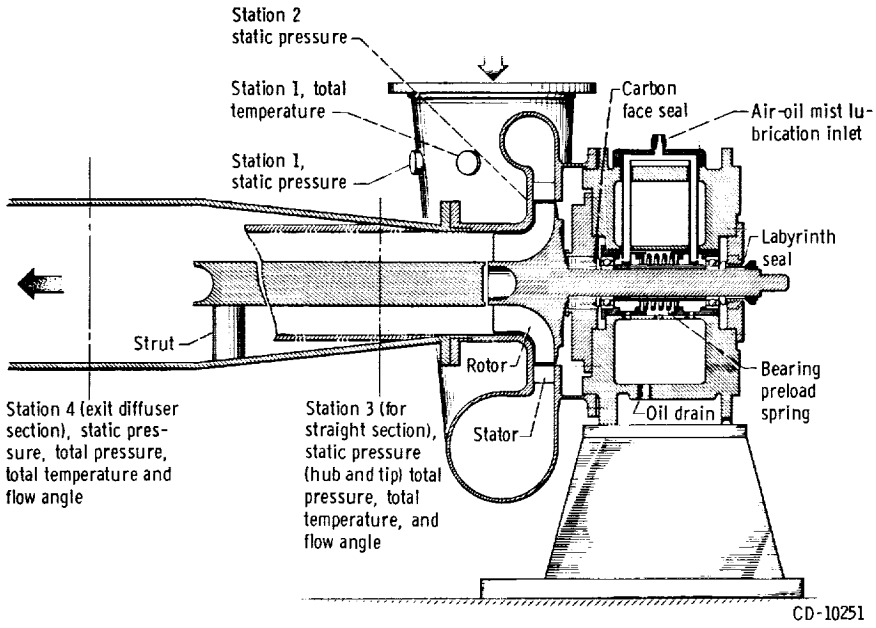

Figure 3. - Turbine instrumentation stations.

ity distributions were satisfactory since there was no large diffusion on either the suction or pressure surfaces. The figure shows that the tip was the most heavily loaded section. The discontinuity in velocities at the exit of the rotor section containing the splitter vanes results from the inability of the calculational method to adjust for flow patterns in this region. In actual operation, however, the sharp discontinuity in velocities does not exist.

Turbine Assembly

A cross-sectional view of the turbine assembly is shown in figure 3. The station numbers are also indicated on this figure.

The rotor exducer at the exit had a tip diameter of 3.460 inches (8.788 cm) and a hub diameter of 1.822 inches (4.628 cm). This results in a hub- to tip-radius ratio of 0.526. The average tip clearance (radial and axial) was 0.010 inch (0.025 cm). A photograph of the rotor and scroll-stator assembly is shown in figure 4.

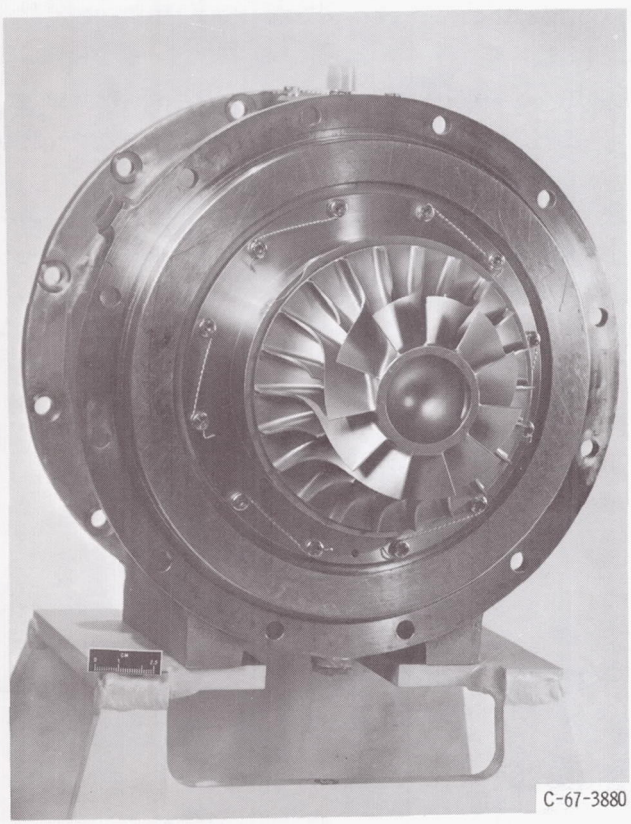

(a) Rotor and bearing housing.

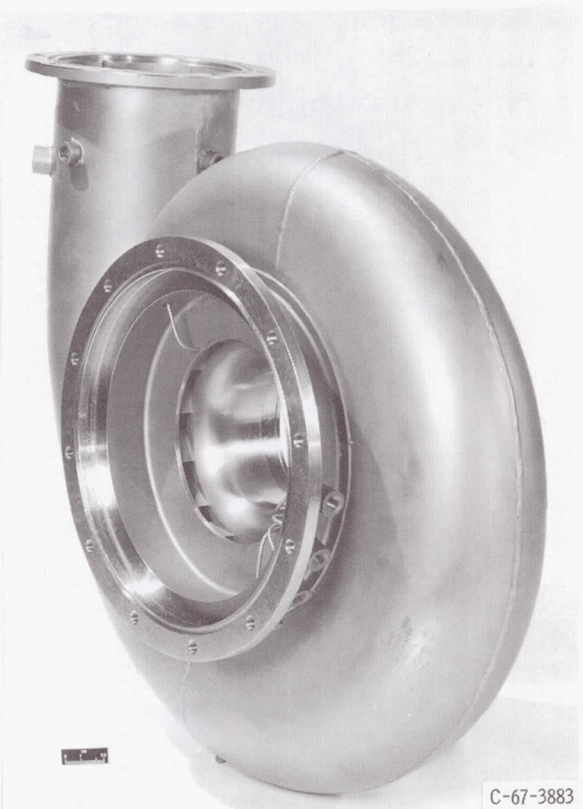

(b) Scroll-stator assembly.

Figure 4. - Rotor and scroll-stator assembly.

The diffuser had an annular inlet area of 6.989 square inches (45.090 cm^2) and an annular exit area of 18.334 square inches (118.284 cm^2). The diffuser was designed to diffuse at a rate consistent with a 5.7^o half-angle conical diffuser.

APPARATUS, INSTRUMENTATION, AND PROCEDURE

Apparatus

The apparatus consisted of the turbine, described in the preceding section, an airbrake dynamometer to absorb and measure the power output of the turbine, and an inlet and exhaust piping system with flow controls. The arrangement of the apparatus is shown schematically in figure 5. Pressurized argon was used as the driving fluid for the turbine. The argon was piped to the turbine through an electric heater, a filter, a weight-flow measuring station consisting of a calibrated flat-plate orifice, and a remotely controlled pressure-regulating valve. The gas, after passing through the turbine, was exhausted through a system of piping and a remotely operated valve into the laboratory low-pressure exhaust system. With a fixed inlet pressure, the remotely operated valve in the exhaust line was used to obtain the desired pressure ratio across the turbine.

The airbrake dynamometer, which was cradle mounted on air bearings for torque measurement, absorbed the power output of the turbine and, at the same time, controlled

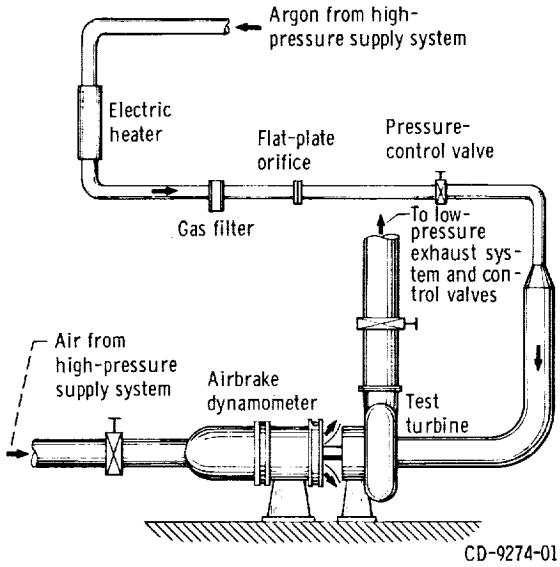

Figure 5. - Schematic of experimental equipment.

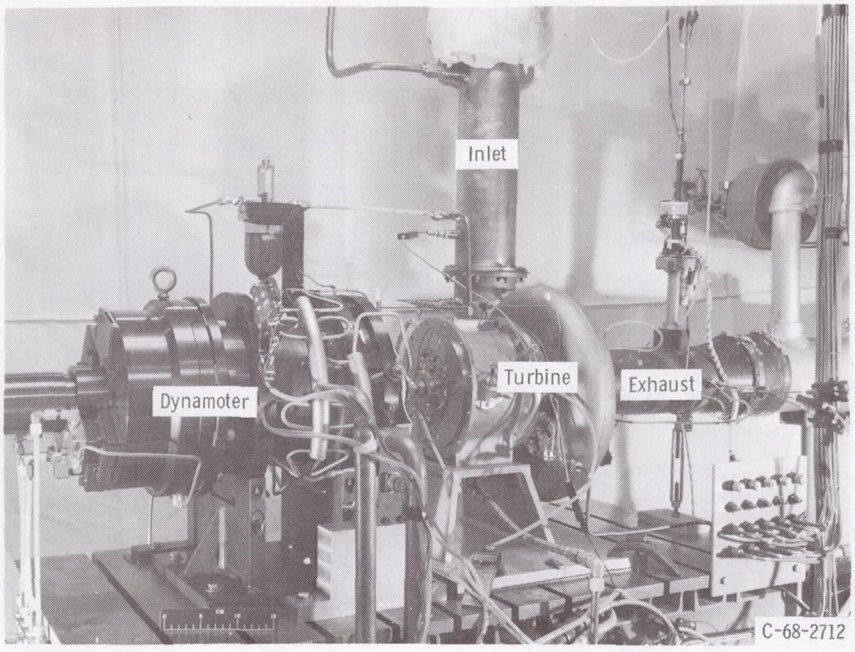

Figure 6. - Installation of turbine in turbine-component test facility.

the speed. The force on the torque arm was measured with a commercial strain-gage load cell. The rotational speed was measured with an electronic counter in conjunction with a magnetic pickup and a shaft-mounted gear. The turbine test facility is shown in figure 6.

Instrumentation

The instrumentation stations are shown in figure 3. Turbine performance was determined by measurements taken at stations 1 and 3 while overall performance was determined by measurements taken at stations 1 and 4. The following instrumentation was located at the turbine inlet (station 1): four static-pressure taps and a total-temperature rake containing three thermocouples. At station 3, downstream of rotor exit and in the annular exit section, the instrumentation consisted of eight static-pressure taps (four each at the inner and outer walls) and a self-alining probe for flow angle, total-temperature, and total-pressure measurements. In the calculation of pressure ratio across the turbine, pressure at station 3 was determined from the average of the static pressures at the inner and outer walls. At station 4, the diffuser exit, the instrumentation consisted of four static-pressure taps on the outer wall and a self-alining probe for flow angle, total-temperature, and total-pressure measurements. Two

interstage pressure taps were installed at station 2 (stator exit) thereby making it possible to determine the variation of static pressure through the turbine.

The values of the absolute pressures at the various stations were measured by electrical transducers. The data were recorded by integrating digital equipment.

Procedure

Three series of tests were made. The first series of tests was made at design Reynolds number with a straight annular section at the rotor exit for determination of turbine performance. The second series of tests at design Reynolds number was made with the annular diffuser for determination of overall (flange to flange) performance. The third series of tests was made over a range of inlet pressures to determine the effect of Reynolds number on turbine as well as overall performance.

Performance data at design Reynolds number were taken at nominal inlet total conditions of 610° R (339 K) and 7.0 psia (4.8 N/cm^2 abs). These values of temperature and pressure correspond to a Reynolds number of about 75 500 at design operation. Data were obtained over a range of equivalent total- to static-pressure ratios from 1.33 to 2.01 and a speed range from 0 to 110 percent of equivalent design. For the Reynolds number tests, the range of inlet pressures was from 2.95 to 16.40 psia (2.03 to 11.31 N/cm^2 abs). Data were obtained over a range of equivalent total- to static-pressure ratios from 1.41 to 1.95 at equivalent design speed.

Friction torque of the bearings and seals was obtained by measuring the amount of torque required to rotate the shaft and rotor over the range of speeds covered in the investigation. In measuring the friction torque, windage losses were minimized by evacuating the air from the turbine to a pressure of about 50 micrometers of mercury (6.667×10^{-4} N/cm^2 abs). A friction torque value of approximately 0.79 inch-pound (0.09 N-m) was obtained at equivalent design speed. This value corresponds to 6.7 percent of the turbine torque obtained at equivalent design-point operation. Friction torque was added to shaft torque when turbine efficiency was determined.

The turbine was rated on the basis of both total and static efficiency. The total pressures were calculated from weight flow, static pressure, total temperature, and flow angle from the following equation:

$$p' = p\left\{\frac{1}{2} + \frac{1}{2}\left[1 + \frac{2(\gamma-1)}{\gamma}\,\frac{R}{g}\left(\frac{w\sqrt{T'}}{pA\cos\alpha}\right)^2\right]^{1/2}\right\}^{\gamma/\gamma-1}$$

In the calculation of turbine-inlet total pressure, the flow angle was assumed to be zero.

RESULTS AND DISCUSSION

Performance results are first presented for operation at design Reynolds number and based on conditions at both the rotor and diffuser exits. A second section presents the internal flow characteristics at design Reynolds number as determined from the measured static-pressure variation through the turbine and the rotor exit radial survey of flow angle, total temperature, and total pressure. A third section shows the effect of a change in Reynolds number on the performance of the turbine with and without the diffuser. All data, with the exception of the radial surveys, are shown in terms of air equivalent values. Blade-jet speed ratio in every case is based on turbine-inlet-total and rotor exit-static conditions.

Performance at Design Reynolds Number

The equivalent specific work output $\Delta h/\sqrt{\theta_{cr}}$ is shown in figure 7 as a function of equivalent pressure ratio $(p'_1/p_3)_{eq}$ for lines of constant speed. The curves show trends similar to those of other radial turbines that have been investigated for a similar space-power application. For the range covered in the investigation, any increase in

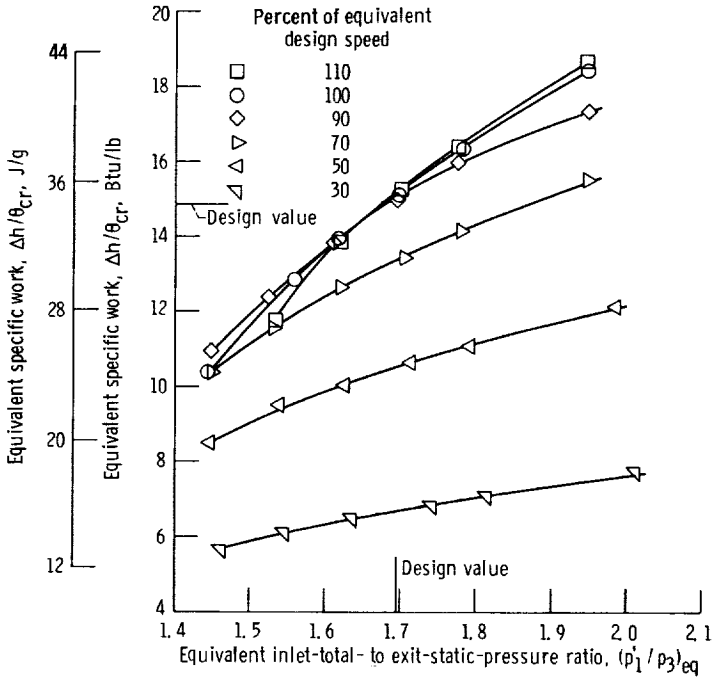

Figure 7. - Variation of specific work with pressure ratio and speed.

pressure ratio results in an increase in specific work at all speeds. Thus, it is shown that the turbine has not reached the point of limiting loading. A value of 15.22 Btu per pound (35.43 J/g) was obtained at equivalent design speed and pressure ratio. This value is 2.7 percent greater than the design value of 14.82 Btu per pound (34.50 J/g).

Mass flow characteristics are shown in figure 8. In this figure mass flow $\epsilon w\sqrt{\theta_{cr}}/\delta$ is plotted as a function of pressure ratio $(p_1'/p_3)_{eq}$ for each of the six speeds. The resulting curves are typical of subsonic turbines in that there is an increase in mass flow with an increase in pressure ratio at all speeds. At equivalent design speed and

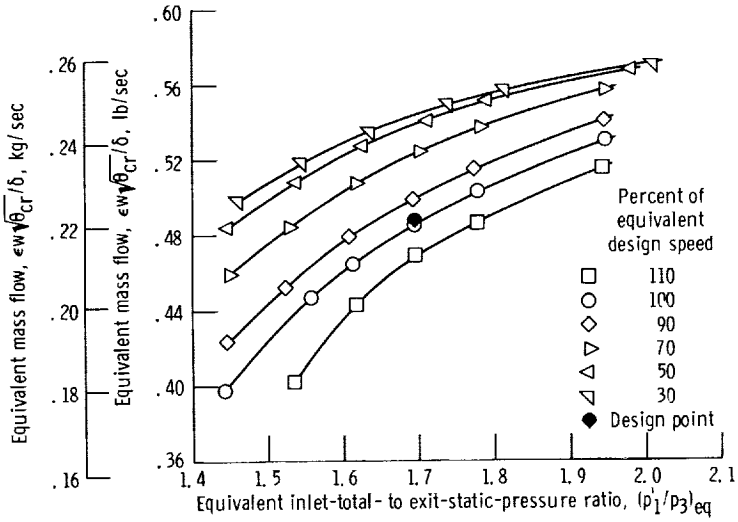

Figure 8. - Variation of mass flow with pressure ratio and speed.

pressure ratio, the mass flow was 0.485 pound per second (0.220 kg/sec), which is nearly identical to the design value of 0.4860 pound per second (0.2204 kg/sec).

The torque $\tau\epsilon/\delta$ is presented in figure 9 as a function of speed and pressure ratio. The values of torque were obtained from faired curves because the data were taken at constant blade speeds and not at constant pressure ratio. The torque at equivalent design speed and pressure ratio was 22.20 inch-pounds (2.51 N-m). This value is about 2.6 percent larger than the design value of 21.64 inch-pounds (2.44 N-m) and about 56 percent of that obtained at zero speed and design pressure ratio. The curves are typical of those for radial inflow turbines in that they deviate appreciably from straight lines. As discussed in reference 8, this deviation is attributed to increased losses when operating at off-design conditions. In figure 10 torque is expressed in the form of a parameter $\eta/\sqrt{2}\,\nu$ and is plotted as a function of blade-jet speed ratio. The nonlinearity between torque and speed as noted in figure 9 is also apparent in this figure.

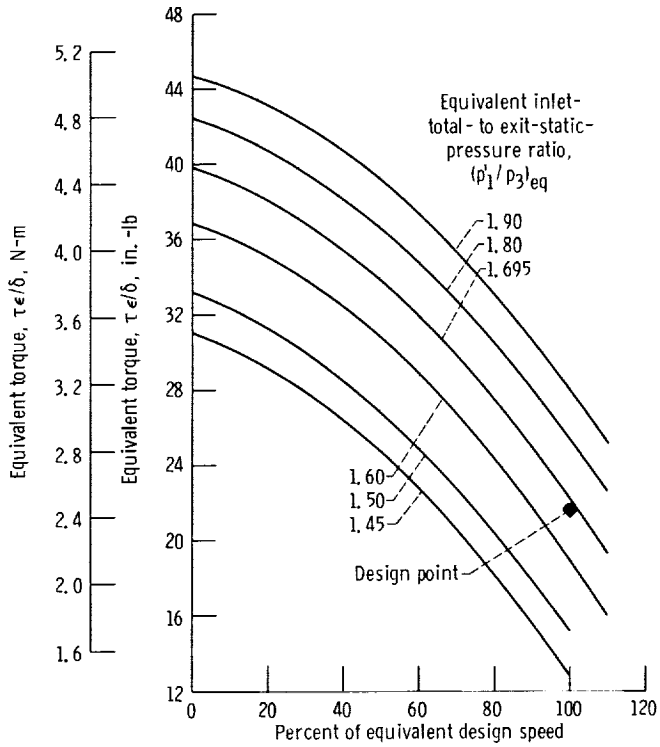

Figure 9. - Variation of torque with speed and pressure ratio.

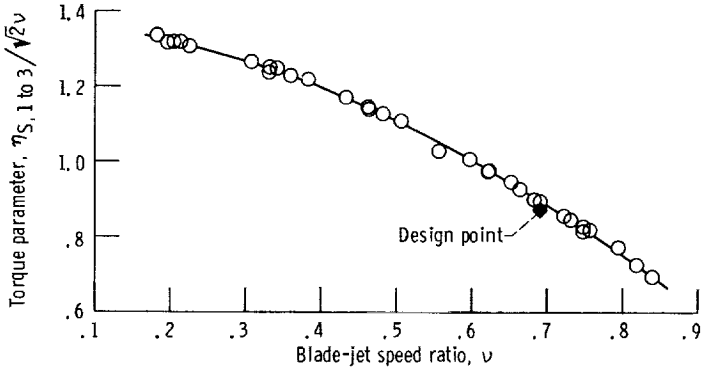

Figure 10. - Variation of torque parameter with blade-jet speed ratio.

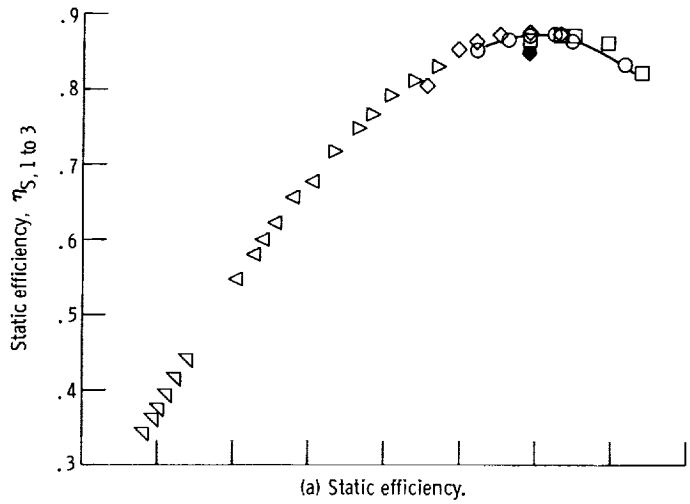

(a) Static efficiency.

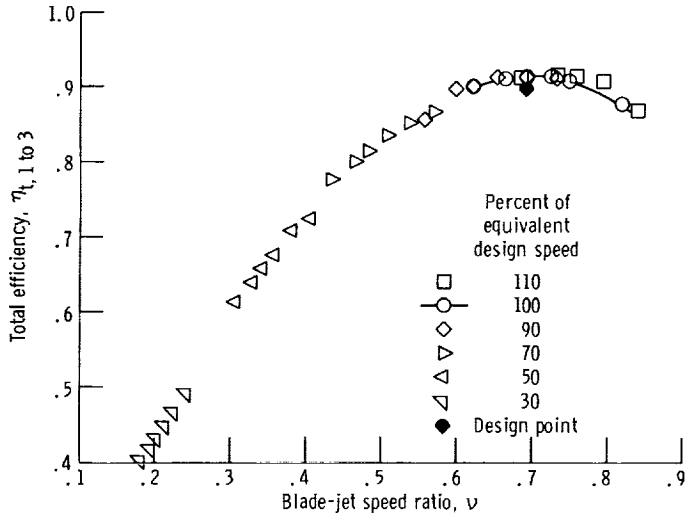

(b) Total efficiency.

Figure 11. - Variation of efficiency (based on rotor-exit conditions) with blade-jet speed ratio.

Figure 11 shows the performance of the turbine from inlet to rotor exit expressed in terms of static and total efficiencies. Efficiency is plotted as a function of blade-jet speed ratio for the six values of speed covered in the investigation. Values of static efficiency of 0.872 (fig. 11(a)) and total efficiency of 0.913 (fig. 11(b)) were obtained at equivalent design-point operation. These values are both about 0.02 higher than the respective design values.

The overall performance of the turbine (including the diffuser) is presented in figure 12 in terms of static and total efficiencies. At design operation, the static efficiency of 0.888 (fig. 12(a)) and the total efficiency of 0.894 (fig. 12(b)) are both about 0.01 higher than their design values.

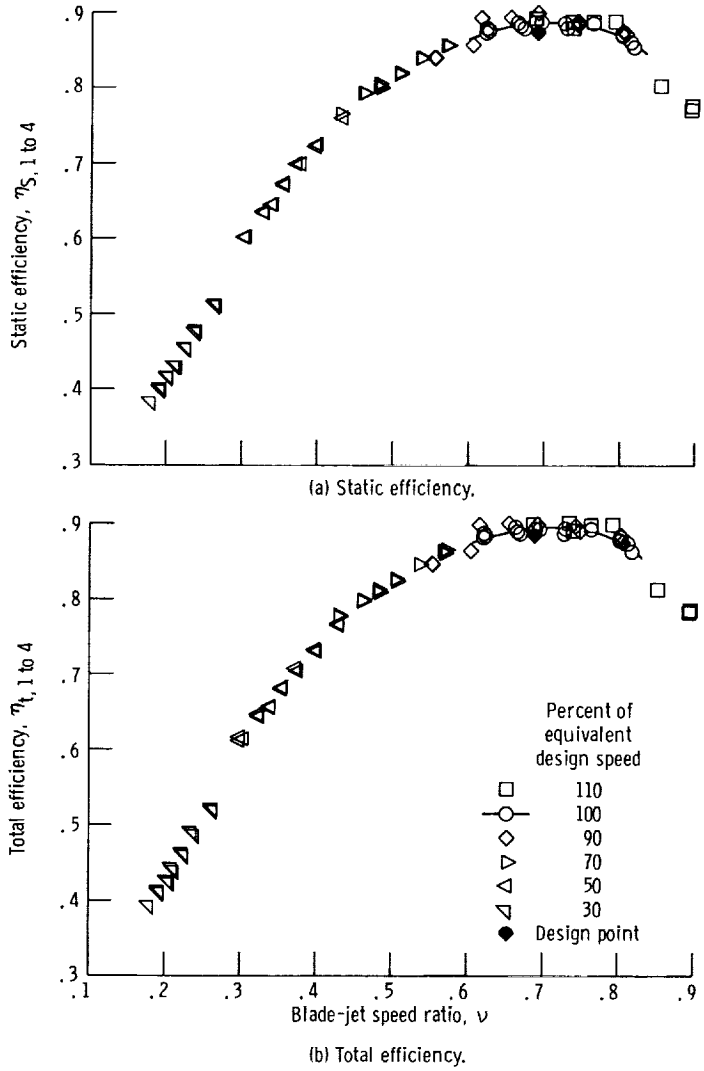

Figure 12. - Variation of efficiency (based on diffuser exit conditions) with blade-jet speed ratio.

Performance results for design-point operation and at design Reynolds number are given in table I along with the design values. Comparison of experimental efficiencies with and without the diffuser (table I) shows a loss in total efficiency with the diffuser of about 0.02 and an increase in static efficiency of about 0.015.

Diffuser performance is commonly expressed in terms of a pressure recovery parameter which is the ratio of static-pressure rise through the diffuser to the diffuser-inlet-impact pressure. Diffuser efficiency as used herein will be defined as the ratio of this parameter to the same parameter for isentropic incompressible diffusion with the same area ratio. The efficiency of the diffuser as calculated from the experimental data was 0.47, which is much lower than the design value of 0.71. Even though the

TABLE I. - PERFORMANCE VALUES

Performance parameters	Design	Experimental
Total efficiency, $\eta_{t,\ 1\ to\ 3}$	0.897	0.913
Static efficiency, $\eta_{s,\ 1\ to\ 3}$	0.850	0.872
Overall total efficiency, $\eta_{t,\ 1\ to\ 4}$	0.884	0.894
Overall static efficiency, $\eta_{s,\ 1\ to\ 4}$	0.875	0.888
Equivalent specific work, $\Delta h/\theta_{cr}$, Btu/lb; J/g	14.82; 34.50	15.22; 35.43
Equivalent mass flow, $\epsilon w\sqrt{\theta_{cr}}/\delta$ lb/sec; kg/sec	0.4860; 0.2204	0.485; 0.220
Equivalent torque, $\tau\epsilon/\delta$, in.-lb; N-m	21.64; 2.44	22.20; 2.51

performance of the diffuser was poor, the overall performance level of the turbine was still better than design.

Internal Flow Characteristics

A description of the internal flow characteristics is based on measured stator-exit static pressures and a rotor-exit radial survey of flow angle, total temperature, and total pressure.

At equivalent design speed and at design pressure ratio, the ratio of stator-exit static pressure to inlet total pressure was 0.763 compared with the design value of 0.783. This indicates an overexpansion of flow across the stator and reduced reaction across the rotor. However, it is apparent from the results already presented that the performance of the turbine at equivalent design speed and pressure ratio was effected very little by the slight deviation from the design velocity diagrams.

The results of a radial survey of turbine exit total pressure, total temperature, and flow angle obtained at design-point conditions are shown in figure 13. The variation of exit total pressure with radius ratio is presented in figure 13(a). There was less than 1 percent deviation from the design value across the passage with the smallest values being recorded in the hub region.

Rotor exit flow angle is shown in figure 13(b) as a function of radius ratio. (Positive angles indicate a flow velocity with a component in the direction of rotation.) Also shown in the figure are the design values at three radial positions. Comparison of the experimental data with the design values shows there was underturning of the flow over

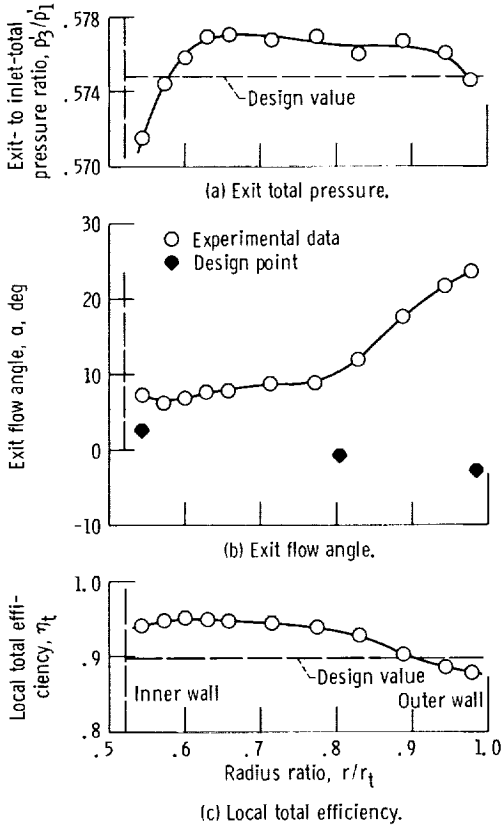

Figure 13. - Variation of rotor-exit total pressure, flow angle, and local total efficiency with radius ratio of design-point operation.

the entire blade height, this result being especially pronounced in the tip region. Even though the flow was underturned at the rotor exit, the specific work obtained was 2.7 percent greater than design as mentioned in the section Performance at Design Reynolds Number. It is thus indicated that the rotor-inlet tangential momentum was greater than design.

In order to obtain more quantitative information, calculations were made to determine the magnitude of the inlet tangential momentum. The mass-averaged exit tangential momentum was determined from calculations involving the rotor-exit survey data and exit static pressures. With this mass-averaged exit tangential momentum value, the rotor-inlet tangential momentum was calculated to satisfy measured specific work. The results of these calculations showed that the rotor-inlet tangential momentum was approximately 10.5 percent larger than the design value.

The very pronounced radial variation in rotor exit flow angle with the large deviation from the design values (fig. 13(b)) suggests a nonuniform work distribution over the blade height. Accordingly, calculations were made to determine the values of total

efficiency at each of the radial positions where data were obtained. These values of local total efficiency were calculated on the basis of the change in tangential momentum through the rotor and the measured values of total pressure at the rotor exit. Figure 13(c) shows values of local total efficiency as a function of radius ratio. The efficiencies in the region of the inner wall are about 0.05 greater than design and about 0.07 greater than those near the outer wall. This variation in efficiency over the blade height is in good agreement with that obtained from measured rotor exit total temperature and may be attributed to secondary flows and/or a blade tip region, which is more heavily loaded than the hub region. It is apparent that specific work in excess of the design value was obtained over the greater part of the blade height.

Performance Over Range of Reynolds Number

Performance results indicated a small effect of Reynolds number on mass flow rate. An increase in Reynolds number from 34 950 to 175 800 resulted in an increase in equivalent mass flow of 1.4 percent at equivalent design speed and pressure ratio. Static-pressure measurements indicated the stator-pressure ratio to be independent of Reynolds number. It is inferred that the increase in mass flow with an increase in Reynolds number was due to decreased viscous losses in the stator and rotor, the ratio between the losses in the stator and rotor remaining the same.

The variation of efficiency without Reynolds number at equivalent design speed and pressure ratio is presented in figure 14. Curves are shown for static and total efficiencies based on conditions at both the rotor and diffuser exits. This figure is the result of cross plots and, accordingly, does not show any actual data points. All curves show similar trends, with an increase in efficiency of about 0.035 for the increase in Reynolds number covered by this investigation. Based on conditions at the rotor exit, total efficiency increased from about 0.890 to 0.925 with a corresponding increase in static efficiency from approximately 0.850 to 0.885.

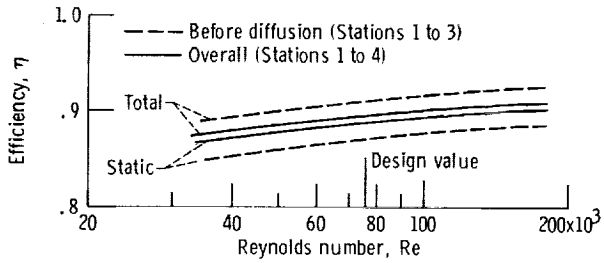

Figure 14. - Effect of Reynolds number on turbine efficiency at equivalent design speed and pressure ratio.

SUMMARY OF RESULTS

An experimental investigation of a 4.97-inch (12.62-cm) tip diameter radial-inflow turbine is presented. This turbine was designed for a single-shaft Brayton cycle space-power system with a helium-xenon gas mixture as the working fluid and a net power level of 6.0 kilowatts (electrical). Performance characteristics using cold argon were obtained at an inlet pressure of 7.0 psia (4.8 N/cm^2 abs) corresponding to design Reynolds number. Additional tests were made to include a range of inlet pressures from 2.95 to 16.40 psia (2.03 to 11.31 N/cm^2 abs), corresponding to a Reynolds number range from 34 950 to 175 800 at equivalent design speed and pressure ratio. Data were obtained both with and without an exit diffuser. The pertinent results of the investigation are as follows:

1. Equivalent specific work of 15.22 Btu per pound (35.43 J/g) was obtained near design Reynolds number (76 200) and at equivalent design speed and inlet-total- to rotor-exit-static-pressure ratio. This value is 2.7 percent greater than the design value of 14.82 Btu per pound (34.50 J/g). Equivalent design mass flow of 0.486 pound per second (0.2200 kg/sec) was obtained at equivalent design speed and pressure ratio.

2. Static and total efficiencies at design-point operation and based on turbine-inlet and rotor-exit conditions were 0.872 and 0.913, respectively. These efficiencies are approximately 0.02 greater than the respective design values.

3. Calculations based on turbine-inlet and diffuser-exit conditions indicated static and total efficiencies of 0.888 and 0.894, respectively. Thus, pressure changes in the diffuser reflected an increase of about 0.015 in static efficiency and a decrease of about 0.02 in total efficiency from their respective values, when based on rotor-exit conditions. These results indicate a diffuser efficiency of 0.47 which is much lower than the design target of 0.71. Even though the performance of the diffuser was poor, the overall performance level of the turbine was still better than design.

4. Both static and total efficiencies increased about 0.035 at equivalent design speed and pressure ratio as the Reynolds number increased from 34 950 to 175 800.

Lewis Research Center,
National Aeronautics and Space Administration,
Cleveland, Ohio, December 31, 1968,
120-27-03-56-22.

REFERENCES

1. Kofskey, Milton G.; and Holeski, Donald E.: Cold Performance Evaluation of a 6.02-Inch Radial Inflow Turbine Designed for a 10-Kilowatt Shaft Output Brayton Cycle Space Power Generation System. NASA TN D-2987, 1965.

2. Holeski, Donald E.; and Futral, Samuel M., Jr.: Experimental Performance of a 5-Inch Single-Stage Axial-Flow Turbine Designed for a Brayton Cycle Space Power System. NASA TM X-1666, 1968.

3. Tysl, Edward R.; Ball, Calvin L.; Weigel, Carl; and Heidelberg, Laurence J.: Overall Performance In Argon of a 6-Inch Radial-Bladed Centrifugal Compressor. NASA TM X-1622, 1968.

4. Kofskey, Milton G.; and Nusbaum, William J.: Aerodynamic Evaluation of Two-Stage Axial-Flow Turbine Designed for Brayton-Cycle Space Power System. NASA TN D-4382, 1968.

5. Vanco, Michael R.: Analytical Comparison of Relative Heat-Transfer Coefficients and Pressure Drops of Inert Gases and Their Binary Mixtures. NASA TN D-2677, 1965.

6. Anon: Design and Fabrication of the Brayton Cycle High Performance Turbine Research Package. Rept. APS-5281-R, AiResearch Mfg. Co. of Arizona, (NASA CR-72478), 1968.

7. Katsanis, Theodore: Use of Arbitray Quasi-Orthogonals for Calculating Flow Distribution in the Meridional Plane of a Turbomachine. NASA TN D-2546, 1964.

8. Futral, Samuel M., Jr.; and Wasserbauer, Charles A.: Off-Design Performance Prediction with Experimental Verification for a Radial-Inflow Turbine. NASA TN D-2621, 1965.

NASA-Langley, 1969 —— 3 E-4715